Solving interactions between nonlinear resonators

Joël Bensoam, David Roze
IRCAM - CNRS UMR 9912, Instrumental Acoustics team, 1 place Igor Stravinsky, F-75004 Paris
joel.bensoam@ircam.fr david.roze@ircam.fr

ABSTRACT

In the context of musical acoustics, physical models of musical instruments have to be more and more sophisticated. For string models, realism is obtained by taking into account tension, flexion, shear, rotation and coupling phenomena but also nonlinear effects due to large displacements. The sound synthesis modal method is extended to the nonlinear case using Volterra series. The inverse problem of interaction between two acoustical objects is solved by finding the roots of a polynomial at each time step.

1. INTRODUCTION

Modalys, a sound synthesis software developed at Ircam for research and musical applications, makes it possible to build virtual instruments based on physical models in order to obtain the broadest range of expressive variations in the instrument in response to intuitive controls. An instrument, as a complex structure, is described by the mechanical/acoustical interactions of its components (strings, tubes, soundboard, 3D FEM objects...). Propagation equations of each substructure are projected on the basis of its modes of vibration, which allows to obtain an infinite dimensional system of differential equations (time dependent). Limiting development in the first predominant modes (in practice, tens or hundreds modes), the system of equations becomes finite and provides a mathematical representation of the behaviour of a substructure irrespective of its nature: mechanical or acoustic. As a result, knowing the nonlinear coupling terms between each substructure, it is possible to characterise the dynamic behaviour of the overall system by assembling these elementary systems of equations. The use of this model requires therefore to have

- a solution for wave propagation (direct problem) in each substructure (depending on initial conditions and external actions),
- interaction models (which depend on the physical situation: contact, friction, reed model, lips, turbulent jet, ...) characterising the connection between substructures

Although, historically, the first stage of this sound synthesis process was done in the linear framework, the purpose of this article is to show that non-linear models can also be used in that context.

So, the linear framework for propagation is recalled in section 2 in order to be extended to the non-linear case (section 3). The mechanism of interaction will not be changed and used to produce an example in the last section.

2. SUBSTRUCTURE SOUND SYNTHESIS

2.1 Green formalism

Since each sub-structure is described by a linear model, a Green operator exists and allows to express the velocity vector field (or displacement field) as a function of applied forces. Formally [1], the wave propagation is obtained by

$$\mathbf{u}(\mathbf{x},t) = \int \mathbb{G}(\mathbf{x},\mathbf{y},t) * f(\mathbf{y},t)\,\mathrm{d}\mathbf{y} \tag{1}$$

which gives, in the numerical point of view, discrete instantaneous linear equations

$$u_i(t_i) = \tilde{u}_i(t_i)_{\to 0} + \sum_j \mathbb{G}_{ij} f_j(t_i) \tag{2}$$

The term $\tilde{u}_i(t_i)_{\to 0}$ determines the state of the system, at time t_i and at point i, in the absence of applied force at the same moment t_i. It characterises the effects of inertia and elasticity due to previous external actions. With this formulation, it is not necessary to obtain the dynamic evolution of all points $i \in [1,\ldots,N]$ of the system. When there are $m \leq N$ interactions (i.e., at most m interaction forces) the system is reduced to m linear equations of type (2). To solve the $2m$ unknowns, k types of interaction models ($k \leq m$) must be given in order to obtain well-posed problem. Finally, the system of equations (propagation & interaction)

$$\begin{cases} u_i(t_i) = \tilde{u}_i(t_i)_{\to 0} + \sum_{j=1}^{m} \mathbb{G}_{ij} f_j(t_i), & i = 1,\ldots,m \\ f_i = \mathcal{C}_{(k)}(u_i), & i = 1,\ldots,m \end{cases} \tag{3}$$

is in principle resolvable since, as pointed out by the tilde symbol, the historical term $\tilde{u}_i(n)_{\to 0}$ is computable. In the case where the interaction models $\mathcal{C}_{(k)}$ are all linear, solving this problem is trivial. If some models are nonlinear, the problem is more complex and the iterative Uzawa's algorithm for saddle point problem is used [2].

Since the interaction models, $\mathcal{C}_{(k)}$, depend on the physical problem, they are supposed to be given. The problem is to formulate the wave propagation in the form given by (2). This can be done by using, for each sub-structure, a modal decomposition, and a numerical simulation for the dynamic of each mode.

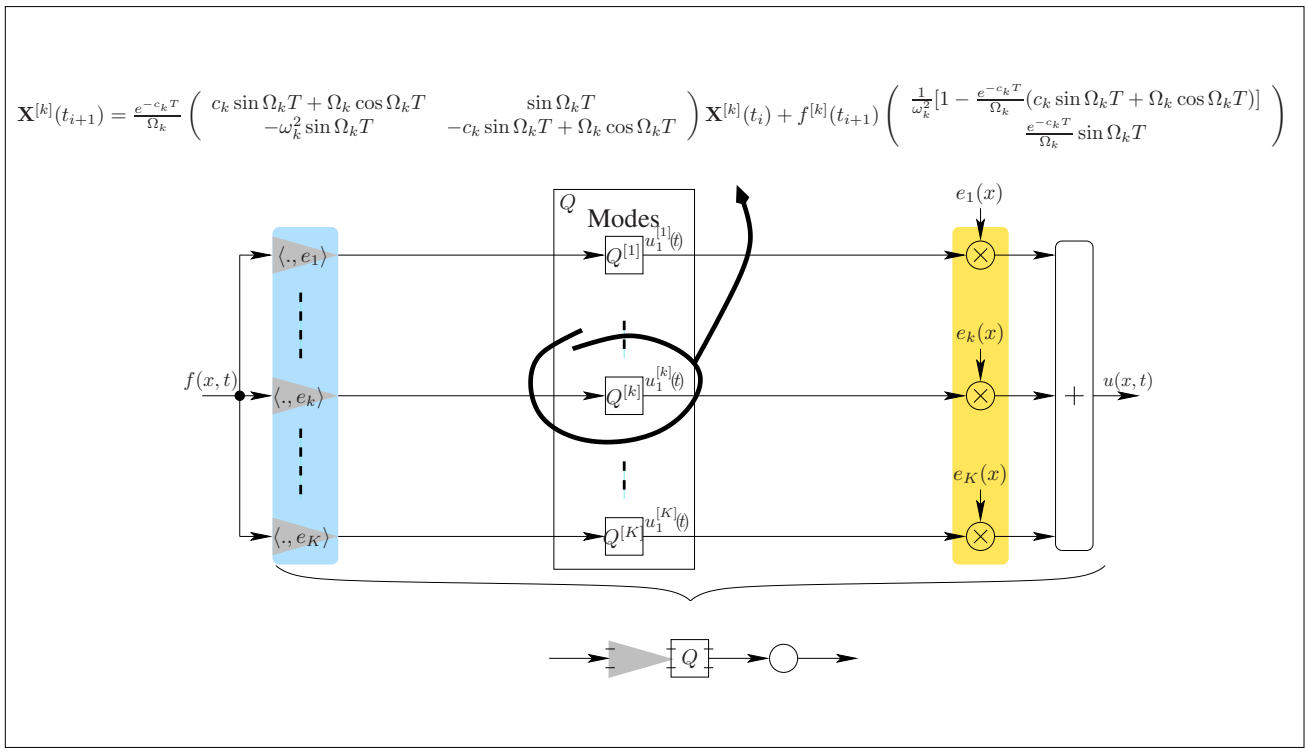

Figure 1. Linear sound synthesis: the propagation equation of each substructure are projected on its modal basis. Limiting the development in the first predominant modes (in practice, tens or hundreds modes), it allows to obtain a finite dimensional system of recursive filters and provides a numerical representation of the behaviour of a substructure irrespective of its nature: mechanical or acoustic.The set Q of filters performs the simulation for K modes. Each filter $Q^{[k]}$ computes a modal output as defined in equation (7) where $\mathbf{X}^{[k]}(t_{i+1})$ is a function of $\mathbf{X}^{[k]}(t_i)$ and input $f^{[k]}(t_{i+1})$ with $\Omega_k = \omega_k \sqrt{1 - \frac{c_k^2}{\omega_k^2}}$.

2.2 Modal synthesis

Given a modal decomposition, $u = \sum_{k=1}^{K} u^{[k]} e_k$, a second order boundary value problem

$$\frac{\partial^2 u}{\partial t^2}(x,t) + 2c(x)\frac{\partial u}{\partial t}(x,t) - \omega^2 \frac{\partial^2 u}{\partial x^2}(x,t) = f(x,t)$$

used to describe a wave propagation, can be written as a set [1] of first order differential equations

$$\begin{cases} \mathbf{X}^{[k]}(t) = \begin{bmatrix} u^{[k]} & \dot{u}^{[k]} \end{bmatrix}^T \\ \dot{\mathbf{X}}^{[k]}(t) = \mathbf{A}^{[k]}\mathbf{X}^{[k]}(t) + \mathbf{B}f^{[k]}(t) \\ \mathbf{A}^{[k]} = \begin{bmatrix} 0 & 1 \\ -\omega_k^2 & -2c_k \end{bmatrix}, \quad \mathbf{B} = \begin{bmatrix} 0 \\ 1 \end{bmatrix} \end{cases} \tag{4}$$

where the matrix $\mathbf{A}^{[k]}$ captures the modal datas (eigen pulsation ω_k, damping c_k), $f^{[k]}$ are the modal forces. This is the state space representation of the filter defined by the transfer function

$$Q^{[k]}(s) = \frac{1}{s^2 + 2c_k s + \omega_k^2}. \tag{5}$$

[1] a modal truncation is performed in order to obtain a finite dimensional set.

Using the exponential map, a solution can be formulated as

$$\mathbf{X}^{[k]}(t) = \int_0^t e^{\mathbf{A}^{[k]}(t-\tau)}\mathbf{B}f^{[k]}(\tau)\mathrm{d}\tau + e^{\mathbf{A}^{[k]}t}\mathbf{X}(0), \tag{6}$$

which gives, after a time discretization: $t_i = iT$ and a zeroth order approximation of the input force, a recursive filter formula

$$\mathbf{X}^{[k]}(t_{i+1}) = e^{\mathbf{A}^{[k]}T}\mathbf{X}^{[k]}(t_i) + \mathbf{B}_0{}^{[k]} f^{[k]}(t_{i+1}) \tag{7}$$

with $\mathbf{B}_0{}^{[k]} = -\mathbf{A}^{[k]^{-1}}\left[\mathbf{B} - e^{\mathbf{A}T}\mathbf{B}\right]$. A modal reconstruction $\sum_k \mathbf{X}^{[k]} e_k$ leads to a formalism in accordance with equation (2). Technically, the computation of the exponential gives rise to a sound synthesis process described in Fig. 1.

3. NONLINEAR WAVE PROPAGATION

Nonlinear wave propagation cannot be computed using the above mentioned tools (modal decomposition and the Green operator) as is. Then, in order to compute interactions between nonlinear resonators a system equivalent to (3) has to be found for the nonlinear case.

This section will introduce the Volterra series used to simulate the dynamics of weakly nonlinear models: a nonlinear equation is turned into an infinity of linear ones for

which the simulation of the dynamics can be handled by the algorithm defined in section 2. The Volterra series can be used for all polynomial nonlinearities around an equilibrium point. This method is not also limited to scalar nonlinearities: fully coupled (transverse/longitudinal) string vibration can also be considered. A Reissner beam model with coupling between the degrees of freedom has been investigated using Volterra series in [6].

To be more pedagogical, only the Kirchhoff-Carrier string model will be used here to illustrate this method.

3.1 Kirchhoff-Carrier string model (KCM)

The equation, defined for $(x,t) \in [0,L] \times \mathbb{R}_+^\star$,

$$\frac{\partial^2 u(x,t)}{\partial t^2} + \delta \frac{\partial u(x,t)}{\partial t} - \kappa \frac{\partial^3 u(x,t)}{\partial t \partial x^2} = \left[c^2 + b \int_0^L \left(\frac{\partial u(x,t)}{\partial x} \right)^2 \mathrm{d}x \right] \frac{\partial^2 u}{\partial x^2} + f_{tot}(x,t) \quad (8)$$

describes the Kirchhoff-Carrier string model [3] [4]. Volterra kernels of this model have been computed in a previous work [5] and simulations were performed. The damping are specified by δ and κ (fluid and structural resp.). The sound speed is c and b is a coefficient of nonlinearity. Boundary conditions are homogeneous Dirichlet conditions (the string motion is null at the edges) and the string is at rest for $t \leq 0$.

3.2 Volterra series

For control engineers, a dynamical system, such as (8), is considered as a causal system with input f and output u (cf. Fig. 2). Using Volterra's series, the solution is defined

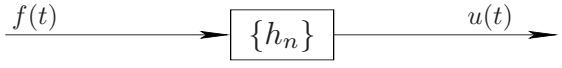

Figure 2. System with input f and output u described by a Volterra series $\{h_n\}_{n\in\mathbb{N}^*}$.

as the infinite sum of multi-convolutions between the input and the Volterra kernels $\{h_n\}_{n\in\mathbb{N}^*}$ of the model

$$u(t) = \sum_{n=1}^{\infty} \int_{(\mathbb{R}^+)^n} h_n(\tau_{1:n}) f(t-\tau_1) \dots f(t-\tau_n) \mathrm{d}\tau_{1:n} \quad (9)$$

with for each (non)linear order n: $(\tau_{1:n}) = (\tau_1, \dots, \tau_n)$ and $\mathrm{d}\tau_{1:n} = \mathrm{d}\tau_1 \dots \mathrm{d}\tau_n$.

More precisely, Volterra's series were historically used to solve ordinary differential equations. Since equation (8) is a partial differential equation, the output of the system is a function of time and space. To respect formulation (9) Volterra kernels will be paremeterized in space and denoted $h_n^{(x)}(t_{1:n})$ in time domain ($H_n^{(x)}(s_{1:n})$ in the Laplace domain) and the input will be split as $f_{tot}(x,t) = \phi(x) f(t)$.

In practice, the simulation will not be performed using this definition of Volterra series, since multi-convolution would be too costly in computation time: First, the explicit expression of Volterra kernels which are a characteristic of the physical system, will be given. Then, a structure of numerical simulation will be made by identifying the Volterra kernels in order to compute the output (transverse displacement) as a function of the input (excitation force).

3.3 Solving the Volterra kernels

One method to find the Volterra kernels is to establish a recursive formula. This procedure is described in [5]§4.1 for the Kirchhoff-Carrier model giving the recurrence relation

$$(\widehat{s_{1:n}}^2 + \delta \widehat{s_{1:n}}) H_n^{(x)}(s_{1:n}) - (c^2 + \kappa \widehat{s_{1:n}}) \frac{\partial^2 H_n^{(x)}(s_{1:n})}{\partial x^2} = E_n^{(x)}(s_{1:n}) \quad (10)$$

where $(\widehat{s_{1:n}}) = (s_1 + \dots + s_n)$. The source $E_n^{(x)}$ is a function of lower order kernels (cf. (12)) and $E_1^{(x)} = \phi(x)$ is the spatial distribution of the input force. Modal decomposition on the modal basis, $e_k(x) = \sqrt{\frac{2}{L}} \sin(\frac{k\pi x}{L})$, is one option to solve the problem (10) by transforming the differential equations into algebraic ones. The modal projection of Volterra kernels then verifies $\forall (n,k) \in (\mathbb{N}^\star)^2$

$$H_n^{[k]}(s_{1:n}) = Q^{[k]}(\widehat{s_{1:n}}) E_n^{[k]}(s_{1:n}) \quad (11)$$

where $Q^{[k]}(s) = \left[s^2 + (\delta + \kappa \frac{k^2\pi^2}{L^2}) s + \frac{k^2\pi^2 c^2}{L^2} \right]^{-1}$ is the transfer function describing the linear part of the model. According to equation (5) each Volterra kernel is a filter where nonlinear effects are contained in the source terms $E_n^{[k]}$. For the particular case of KCM, this yields

$$\begin{cases} E_1^{[k]} = \langle \phi, e_k \rangle = \phi_k \\ E_n^{[k]}(s_{1:n}) = \gamma_k \sum_{\substack{p,q,r \geq 1 \\ p+q+r=n}} \\ \left[\sum_{\ell=1}^K \ell^2 H_p^{[\ell]}(s_{1:p}) H_q^{[\ell]}(s_{p+1:p+q}) \right] H_r^{[k]}(s_{p+q+1:n}), \end{cases} \quad (12)$$

with $\gamma_k = -b \frac{k^2\pi^4}{L^4}$. Thus it can be seen that E_n depends only on the lower order kernels H_p, H_q, H_r since the principal sum is over $p+q+r=n$.

3.4 Structure of simulation based on Volterra kernels

The Volterra kernels are not explicitly computed. In practice, equation (11) is used in the multi-convolution (9) to identify a structure of simulation. This structure is composed of linear filters sets (each one representing a nonlinear order) connected with sums and products according to the combinatorics revealed in (12). To illustrate this, the general structure of this kind of simulation is presented in Fig. 3. To give a concrete realisation Fig. 4 represents this structure for the Kirchhoff-Carrier model limited to the third order: the output approximation has two components, $u(x,t) = u_1(x,t) + u_3(x,t)$ (since there is no quadratic nonlinearity).

The first part (well-known order 1 contribution) is $U_1^{[k]}(s) = H_1^{[k]}(s) F(s) = Q^{[k]}(s) \phi_k F(s)$ where $F(s)$ is the Laplace transform of excitation force $f(t)$. For the second part, knowing from (11) and (12) that

$$H_3^{[k]}(s_{1:3}) = Q^{[k]}(\widehat{s_{1:3}}) E_3^{[k]}(s_{1:3}) = Q^{[k]}(\widehat{s_{1:3}}) \gamma_k \sum_{\ell=1}^K \ell^2 H_1^{[\ell]}(s_1) H_1^{[\ell]}(s_2) H_1^{[k]}(s_3)$$

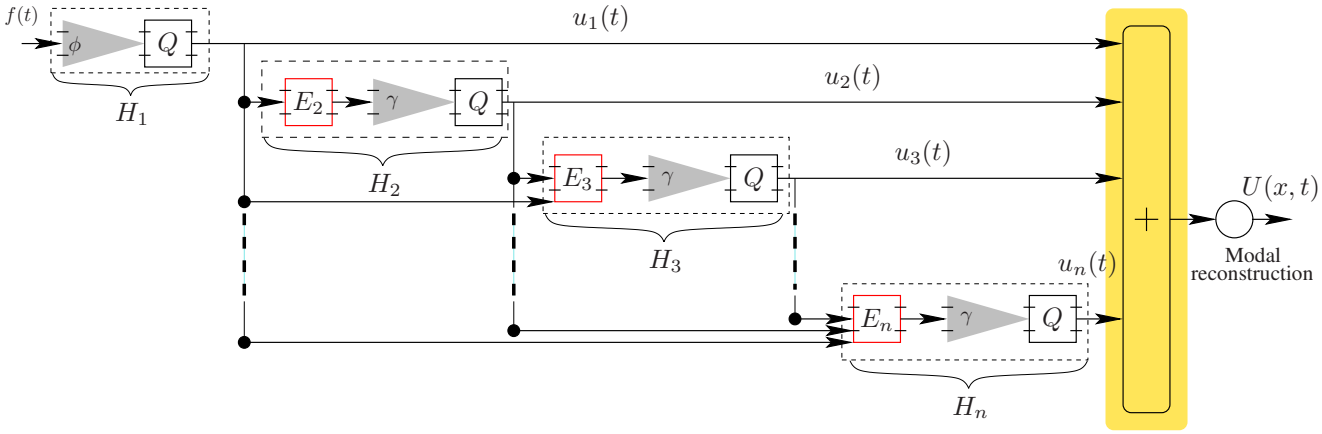

Figure 3. Recursive structure of simulation based on Volterra kernels. Each line represents the K modal projections of u_i. According to equation (11) and Fig. 1, E_i represents the combinatorics of lower order kernels on all K modes in order to compute H_i with the set of filters Q. The triangle γ contains all the nonlinear coefficients γ_k, as ϕ is the set of ϕ_k.

	N=1	N=3
N^f	$K(9+2N_x)-N_x$	$K(2\times 9+2N_x+5)-N_x$

Table 1. Number N^f of floating point operations to compute one sample of $u(x,t)$ with K modes for linear approximation ($N=1$) and third-order approximation ($N=3$) at N_x observation points.

and according to (9), u_3 is computed by

$$\begin{aligned} U_3^{[k]}(s_{1:3}) &= H_3^{[k]}(s_{1:3})F(s_1)F(s_2)F(s_3) \\ &= Q^{[k]}(\widehat{s_{1:3}})\gamma_k \sum_{\ell=1}^{K} \ell^2 H_1^{[\ell]}(s_1)H_1^{[\ell]}(s_2)H_1^{[k]}(s_3) \\ &\qquad F(s_1)F(s_2)F(s_3) \\ &= Q^{[k]}(\widehat{s_{1:3}})\gamma_k \sum_{\ell=1}^{K} \ell^2 U_1^{[\ell]}(s_1)U_1^{[\ell]}(s_2)U_1^{[k]}(s_3) \end{aligned}$$

This last relation gives the structure of simulation presented in Fig. 4 with K modes.

At this point, sound synthesis can then be performed for reasonable computation time: adding one nonlinear component to linear synthesis approximatively doubled the simulation time. Actually, the number of required floating point operations (flops) is evaluated in Table 1 using Fig. 4 and knowing that each filter $q^{[k]}$ requires 4 sums and 5 products (9 flops) for each time sample.

3.5 Green operator based on Volterra kernels

In order to perform sound synthesis and compute interactions with nonlinear resonators represented by Volterra series the algorithm presented in section 2 has to be extended. The relation (2) between force and displacement/velocity which was an affine function will become a polynomial of same order as the truncation of the Volterra series.

To see this, let be the vector $\mathbf{X}_n^{[k]}(t_i) = \begin{bmatrix} u_n^{[k]}(t_i) \\ \dot{u}_n^{[k]}(t_i) \end{bmatrix}$ the state-space representation used in section 2.2 where n is the nonlinear order and k the considerated mode. Since the final desired result is a modal reconstruction of all nonlinear contributions $\mathbf{X}_n^{[k]}$

$$\mathbf{X}(x,t_i) = \sum_{n=1}^{N}\sum_{k=1}^{K} \mathbf{X}_n^{[k]}(t_i)e_k(x), \tag{13}$$

and since according to formula (7) each nonlinear contribution (dotted rectangles in Fig. 3) can be written as

$$\mathbf{X}_n^{[k]}(t_i) = \tilde{\mathbf{X}}_n^{[k]}(t_i) + \mathbf{B}_0^{[k]} f_n^{[k]}(t_i), \tag{14}$$

it follows that the relation between force and displacement is a polynomial

$$\mathbf{X}(x,t_i) = \tilde{\mathbf{X}}(x,t_i) + \Pi(f(t_i)). \tag{15}$$

The modal excitation force $f_1^{[k]}(t_i)$ is the input of the system. For higher orders ($n \geq 2$) the source term $f_n^{[k]}(t_i)$ is a combination of variables $\mathbf{X}_p^{[k]}$ which are already known since the order $p < n$.

This yields for the Kirchhoff-Carrier model studied before (still limited to order $N=3$), the functions $f_1^{[k]}(t_i) = \phi_k f(t_i)$ that handle the modal decomposition of the spatial distribution $\phi(x)$ of the external force. For $n=3$, the terms $f_3^{[k]}(t_i) = \gamma_k \sum_{\ell=1}^{K}(\ell u_1^{[\ell]}(t_i))^2 u_1^{[k]}(t_i)$ (cf. equation (12)) capture the non linear effects due to the deformation of the string. Evaluating equation (14) for $n=1$ and $n=3$ turns equation (13) into an order 3 polynomial

$$\begin{aligned} \mathbf{X}(x,t_i) &= \tilde{\mathbf{X}}(x,t_i) + \mathbf{\Theta}_3(x)f^3(t_i) \\ &+\mathbf{\Theta}_2(x,t_i)f^2(t_i) + \mathbf{\Theta}_1(x,t_i)f(t_i) \end{aligned} \tag{16}$$

where the coefficient are described in appendix A.

Finally, in the general case (N can be higher than 3), the system propagation and interaction for a nonlinear resonator can still be represented by

$$\begin{cases} \mathbf{X}(x,t_i) = \tilde{\mathbf{X}}(x,t_i) + \Pi(f(t_i)) \\ f(t_i) = \mathcal{C}_{(k)}(\mathbf{X}(t_i)) \end{cases} \tag{17}$$

where Π is a polynomial of same order as the nonlinear truncation. This is an extension of the substructure coupling method defined in equation (3) to the nonlinear case.

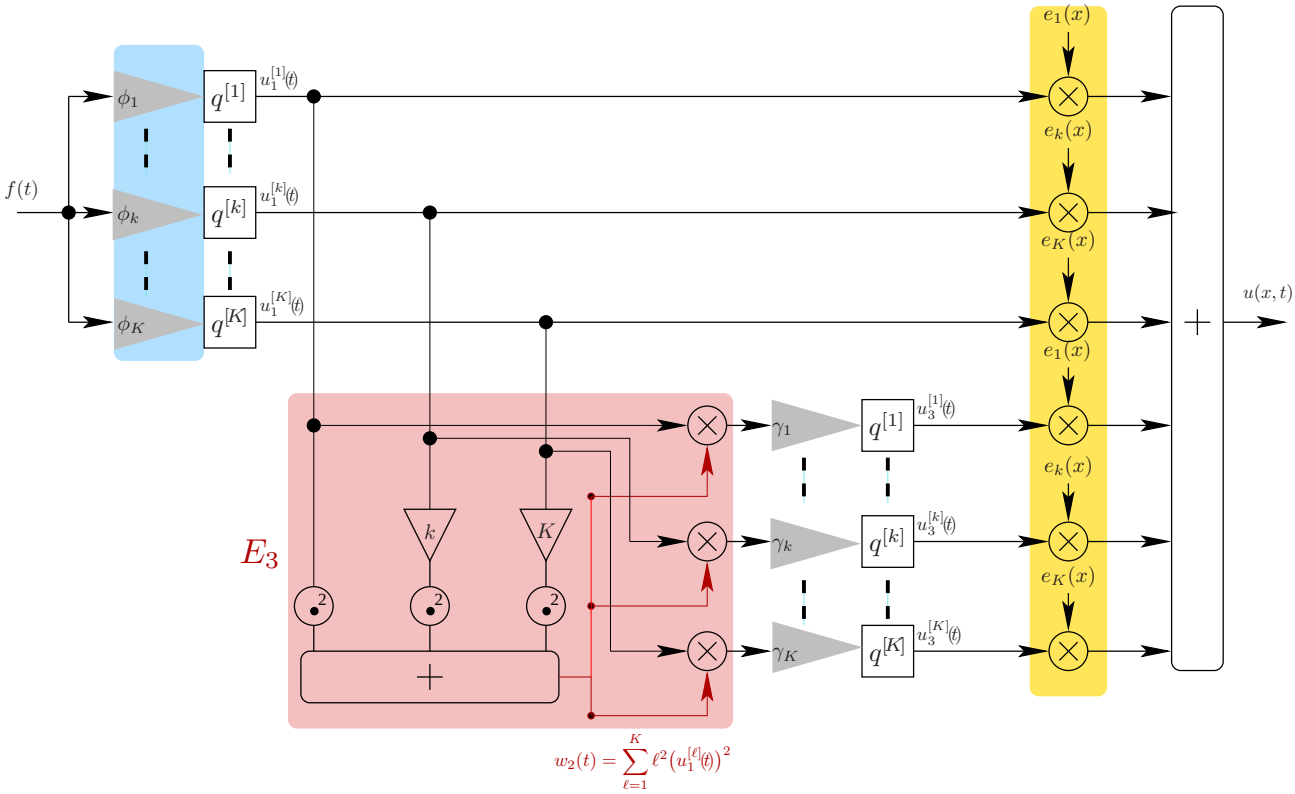

Figure 4. Structure of simulation of the Kirchhoff-Carrier model limited to the third order. Filters in the left column compute the linear response for each mode whereas the second column compute the order 3 response. Triangles are simple gains corresponding to spatial distribution of force for order 1, and nonlinear coefficient for order 3.

4. SIMULATION ON AN INTERACTION EXAMPLE: "ADHERE COUPLING"

In this section, the formalism (17) for propagation *and* interaction between nonlinear resonators is investigated with two strings glued together for a moment then released for free oscillation. In this example, the choice of the coupling $\mathcal{C}$ is shown in figure (9).

4.1 The "Adhere coupling"

When two substructures (here, two nonlinear strings) are glued together, the relative velocity at the interface point vanishes: the model of interaction is then represented by the vertical line in the force/velocity plane (Fig. 9).

Solving the interaction consists in finding the intersection point between this line and the polynomial of relative velocity defined by $v_r(t_i) = \dot{u}_r(t_i) = \dot{u}_a(x_a, t_i) - \dot{u}_b(x_b, t_i)$. For this type of contact where $v_r = 0$, this will gives the equation

$$\tilde{v}_r(t_i) + \Pi_a(f_a(t_i)) - \Pi_b(f_b(t_i)) = 0 \qquad (18)$$

that permits to compute the interaction force f for each time step. Note the sign reversal in the normal force $f_a = -f_b = f$ according to Newton's third law, where f_a (resp. f_b) is the interaction force applied to object A (resp. B). Those resulting forces are then used as inputs to the propagation simulation for the next time step.

	String A	String B
Length	1.8m	1.5m
Frequency	55Hz	68Hz
Interaction point	$\frac{\sqrt{2}}{2} L_A$	$\frac{\sqrt{2}}{2} L_B$
Nonlinear coefficient	$b_A = \frac{E}{2\rho L_A}$	$b_B = \frac{E}{2\rho L_B}$
Damping	$\delta = 3\text{s}^{-1}$, $\kappa = 0.01\text{m}^2\text{s}^{-1}$	
Young modulus	$E = 2.0 \times 10^{11}$Pa	
Material density	$\rho = 7800\text{kg m}^{-3}$	

Table 2. Physical parameters of the two strings used in the simulation.

4.2 Simulation

A simulation has been performed with two strings defined by Kirchhoff-Carrier model, one of them being excited by the force described in Fig. 5.

The strings physical parameters are described in Table 2. The simulation is performed with $K = 20$ modes at a sampling frequency $f_s = 44100$Hz. The interaction duration has been set to 5000 samples. Both strings are observed by a modal reconstruction at interaction points.

Simulation results are presented in Figs. 6 and 7. We can see that the first string (in blue) vibrates freely before the "Adhere interaction" is imposed, then the two strings velocities are equals, the relative error on displacement and velocity can be seen in Fig. 8: the error is lower for velocity than for displacement since, the interaction definition is based only on relative velocity.

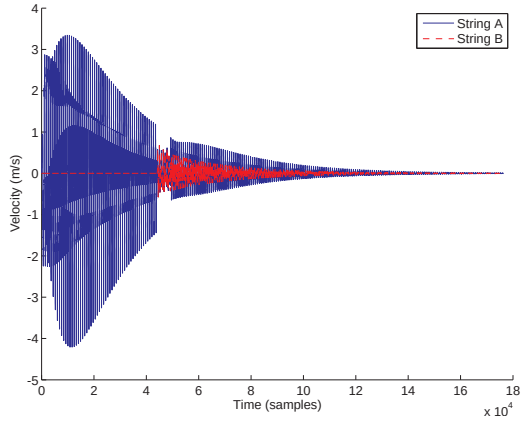

(a) Two strings in interaction: temporal velocity signals

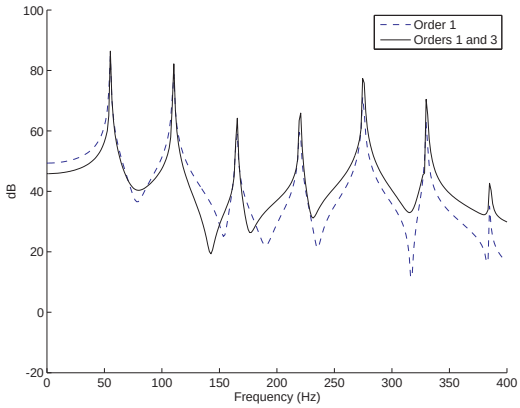

(b) String A spectrum before interaction: taking into account the nonlinearity, a spectral enhancement is obtained

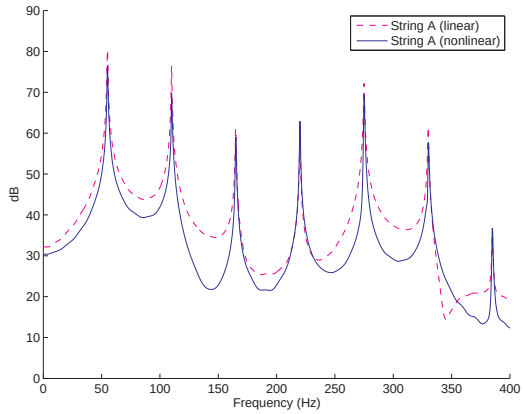

(c) String A spectrum after interaction: nonlinear effects are still present in the dynamics

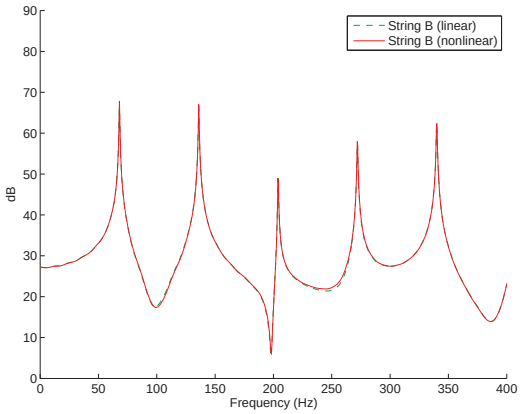

(d) String B spectrum after interaction, the contact force makes string B vibrate.

Figure 7. Interaction between two nonlinear strings: The first string A vibrates freely. An "Adhere coupling"interaction is then applied between the two strings during 5000 samples. The interaction force between the strings A and B, is computed from nonlinear dynamics of the two strings using the two first Volterra kernels. The nonlinear effects are still present in the string A after the interaction. A spectral enhancement can be observed on the spectra before and after the coupling. String B vibrates after the interaction using energy provided by the interaction force.

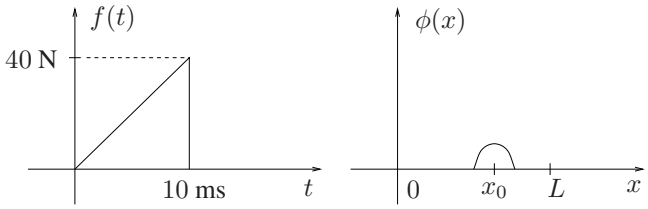

Figure 5. Functions $f(t)$ and $\phi(x)$ used to define the initial excitation force $f_{tot}(x,t) = f(t)\phi(x)$ for the simulation.

After 5000 samples the interaction is removed and the two strings vibrates freely at their own dynamics as shown in Figs. 7(c) and 7(d). This figure shows that for a sufficient excitation force, nonlinear effects appears: the linear and nonlinear part have the same magnitude for the first modes, but for higher frequencies the nonlinear part has an higher magnitude which can be heard in simulations sounds which are more brilliant when the nonlinear contribution is activated. This is noticeable for string A, but not for string B. It can be deduced that the interaction force to string B was not high enough to trigger nonlinear effects.

5. CONCLUSION

This paper introduced an extension of the Green formalism and problem inversion to the case of weakly nonlinear resonators. Using a Volterra series until order N to simulate the dynamics of a string, interactions can be computed the same way the sound synthesis software Modalys does, by solving an order N polynomial instead of a affine function.

The work presented here is based on a particular case where $f(x,t) = \phi(x)f(t)$. The polynomial roots and the convergence of the Volterra series will be studied in a future work before using a more general force $f(x,t)$. Furthermore, it will be possible to consider more realistic string or beam models with polarisation and coupling between transverse and longitudinal displacements and rotations.

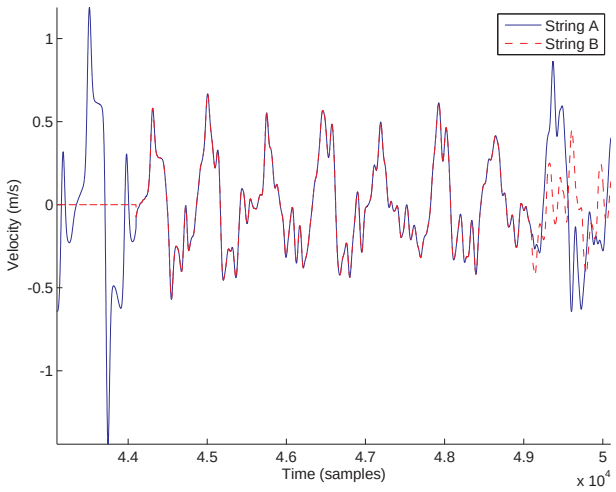

Figure 6. Zoom on the velocity of the two strings during the interaction ($44100 \leq t \leq 49100$ samples). As mentioned in section 4.1 the relative velocity ($v_r = v_A - v_B$) is null during the interaction.

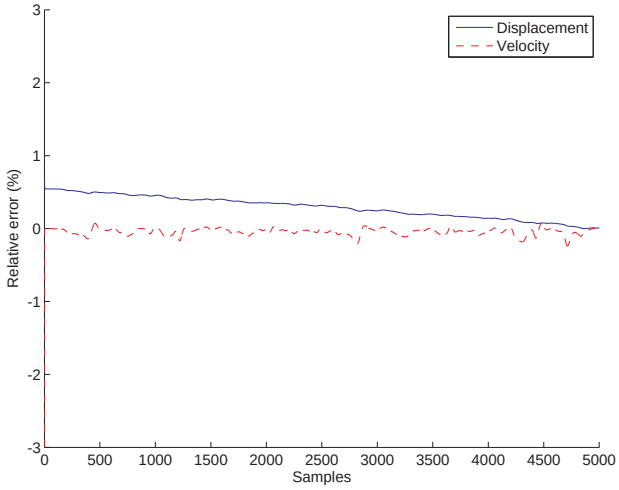

Figure 8. Relative error (for velocity and displacement) between string A and string B during the interaction.

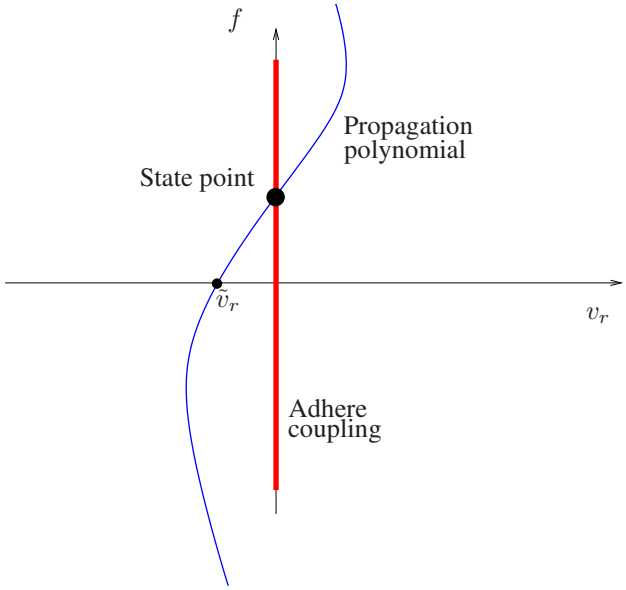

Figure 9. Interaction law (in thick red) for the "Adhere coupling" in the force/velocity plane: relative velocity vanishes when the substructure are glued. The state point is obtained by intersection of this law with the (relative) dynamics of the nonlinear resonators representing by a polynomial (in blue) whose order correspond to the Volterra series truncation order. In case of linear propagation it would be a straight line (first order polynomial).

A. COEFFICIENTS OF THE POLYNOMIAL

The coefficients of the polynomial (16) are

$$\boldsymbol{\Theta}_3^{[k]}(x) = \sum_{k=1}^{K} \gamma_k \mathbf{B}_0^{[k]} \sum_{\ell=1}^{K} (\ell \mathbf{C}\mathbf{B}_0^{[\ell]}\phi_\ell)^2 \mathbf{C}\mathbf{B}_0^{[k]}\phi_k e_k(x)$$

$$\boldsymbol{\Theta}_2^{[k]}(x,t_i) = \sum_{k=1}^{K} \gamma_k \mathbf{B}_0^{[k]} \Bigg[\sum_{\ell=1}^{K} (\ell \mathbf{C}\mathbf{B}_0^{[\ell]}\phi_\ell)^2 \tilde{u}_1^{[k]}(t_i) + \sum_{\ell=1}^{K} 2\ell^2 \tilde{u}_1^{[\ell]}(t_i) \mathbf{C}\mathbf{B}_0^{[\ell]}\phi_\ell \mathbf{C}\mathbf{B}_0^{[k]}\phi_k \Bigg] e_k(x)$$

$$\boldsymbol{\Theta}_1^{[k]}(x,t_i) = \sum_{k=1}^{K} \Bigg[\gamma_k \mathbf{B}_0^{[k]} \Bigg[\sum_{\ell=1}^{K} (\ell \tilde{u}_1^{[\ell]}(t_i))^2 \mathbf{C}\mathbf{B}_0^{[k]}\phi_k + 2\ell^2 \tilde{u}_1^{[\ell]}(t_i) \mathbf{C}\mathbf{B}_0^{[\ell]}\phi_\ell \tilde{u}_1^{[k]}(t_i) \Bigg] + \mathbf{B}_0^{[k]}\phi_k \Bigg] e_k(x)$$

$$\tilde{\mathbf{X}}(x,t_i) = \sum_{k=1}^{K} \Bigg[\tilde{\mathbf{X}}_3^{[k]}(t_i) + \tilde{\mathbf{X}}_1^{[k]}(t_i) + \gamma_k \mathbf{B}_0^{[k]} \sum_{\ell=1}^{K} (\ell \tilde{u}_1^{[\ell]}(t_i))^2 \tilde{u}_1^{[k]}(t_i) \Bigg] e_k(x)$$

with $\mathbf{C} = \begin{bmatrix} 1 & 0 \end{bmatrix}$.

Acknowledgments

We would like to thank the CAGIMA project supported by the National French Research Agency (ANR).

B. REFERENCES

[1] J. Bensoam, "Représentation intégrale appliquée à la synthèse sonore par modélisation physique : méthode des éléments finis," Thèse de doctorat, Académie de Nantes Université du Maine, 2003.

[2] ——, "Mise en oeuvre des couplages non linéaires dans le logiciel de synthèse sonore : Modalys," in *8ème Congrès Français d'Acoustique CFA*, Tours, Avril 2006.

[3] G. Kirchhoff, *Vorlesungen über Mathematische Physik: Mechanik*. Leipzig: Teubner, 1877.

[4] G. F. Carrier, "On the non-linear vibration problem of the elastic string," *Quarterly of Applied Mathematics*, vol. 3, pp. 157–165, 1945.

[5] T. Hélie and D. Roze, "Sound synthesis of a nonlinear string using volterra series," *Journal of Sound and Vibration*, vol. 314, pp. 275–306, 2008.

[6] D. Roze, "Simulation de la propagation d'onde non linéaire par les séries de volterra," Thèse de doctorat, Université Pierre et Marie Curie - Paris VI, 2010.